(22) Reference 14 describes a modification of HMTSeF in which sulfur replaces the β-methylene (i.e., β-DTTSeF).
(23) Other syntheses of HMTTF: (a) E. Fanghänel, L. van Hink, and G. Schukat, *Z. Chem.*, **16**, 317, 360 (1976); (b) H. K. Spencer, M. P. Cava, F. G. Yamagishi, and A. F. Garito, *J. Org. Chem.*, **41**, 730 (1976); P. Delhaes, S. Flandrois, J. Amiell, G. Keryer, E. Toreilles, J. M. Fabre, L. Giral, C. S. Jacobsen, and K. Bechgaard, *J. Phys.*, 233 (1977).
(24) For earlier references on this cyclization see E. Campaigne, R. D. Hamilton, and N. W. Jacobsen, *J. Org. Chem.*, **29**, 1708 (1964); I. D. Rae, *Int. J. Sulfur Chem.*, **1**, 59 (1971); A. K. Bhattacharya and A. G. Hortmann, *J. Org. Chem.*, **39**, 95 (1974), and references cited therein; R. R. Schumaker and E. M. Engler, *J. Am. Chem. Soc.*, **99**, 5521 (1977).
(25) (a) F. Wudl, G. M. Smith, and E. J. Hufnagel, *Chem. Commun.*, 1435 (1970); (b) D. L. Coffen, J. Q. Chambers, D. R. Williams, P. E. Garrett, and N. D. Canfield, *J. Am. Chem. Soc.*, **93**, 2258 (1971); (c) S. Hünig, G. Kiesslich, H. Quast, and D. Scheutzow, *Justus Liebigs Ann. Chem.*, 310 (1973).
(26) E. Klingsberg, *J. Am. Chem. Soc.*, **86**, 5290 (1964).
(27) For the naming of the heterofulvalenes presented in this paper, the 1,4,5,8-tetraheterofulvalene system is chosen as the parent ring.
(28) A convenient, high-yield synthesis of 1,2,3-selenadiazoles has been discovered by I. Lalezari, A. Shafiee, and M. Yalpani, *Tetrahedron Lett.*, 5105 (1969); I. Lalezari, A. Shafiee, and M. Yalpani, *J. Org. Chem.*, **36**, 2836 (1971).
(29) Phosphorus base coupling is currently the only effective means of coupling the selenium analogues of TTF. See ref 17a for discussion. See also ref 11.
(30) E. M. Engler, R. R. Schumaker, and V. V. Patel, *J. Chem. Soc., Chem. Commun.*, 835 (1977).
(31) E. M. Engler and V. V. Patel, *Tetrahedron Lett.*, 423 (1976).
(32) ^{1}H NMR was able to show the presence of cis and trans isomers in DSeDTF (ref 5) and in DMDSeDTF (ref 10).
(33) The crystal structure of β-MeHMTSeF has recently been determined by S. J. LaPlaca, IBM Research (unpublished work). It confirms the presence of the methyl groups in the β positions. In the samples investigated, crystallization apparently has lead to preferential enrichment in the syn isomer.
(34) For earlier references on this cyclization see (a) A. Takamizawa and K. Hirai, *Chem. Pharm. Bull.*, **17**, 1924, 1931 (1969); (b) ref. 8.
(35) For an analogous cyclization involving replacement of oxygen by sulfur see P. Rioult and J. Vialle, *Bull. Soc. Chim. Fr.*, 4478 (1968).
(36) For earlier references on this cyclization see E. Campaigne and N. W. Jacobsen, *J. Org. Chem.*, **29**, 1703 (1964); E. Fanghänel, *Z. Chem.*, **1**, 58 (1967).
(37) A. Roxenbaum, H. Kirchberg, and E. Leibnitz, *J. Prakt. Chem.*, **19**, 1 (1963).
(38) T. Amano, H. Kuroda, and H. Akamatu, *Bull. Chem. Soc. Jpn.*, **41**, 83 (1968); J. B. Torrance, B. A. Scott, and F. B. Kaufman, *Solid State Commun.*, **17**, 1369 (1975).
(39) R. Foster "Organic Charge-Transfer Complexes", Academic Press, New York, N.Y., 1969.
(40) H. K. Spencer, M. P. Cava, and A. F. Garito, *J. Chem. Soc., Chem. Commun.*, 966 (1976).
(41) F. G. Yamagishi, D. J. Sandman, A. F. Garito, and A. J. Heeger, Abstracts, 167th National Meeting of the American Chemical Society, Los Angeles, Calif., March 1973, No. ORGN-12.
(42) R. P. Shibaeva and O. V. Yarochkina, *Sov. Phys. Dokl.*, **20**, 304 (1975).
(43) J. P. Ferraris and F. I. Mopsick, *Chem. Eng. News* (Sept 16, 1974); see also K. G. R. Sundelin, *ibid.* (Aug 5, 1974).
(44) For the preparation of less dangerous hexafluorophosphate salts see L. R. Melby, H. D. Hartzler, and W. A. Sheppard, *J. Org. Chem.*, **39**, 2456 (1974).
(45) L. Henriksen and E. S. S. Kristiansen, *Inst. J. Sulfur Chem., Part A*, **2**, 133 (1972).
(46) C. C. Price and J. M. Jusge, *Org. Synth.*, **45**, 22 (1965).
(47) For an overview of some of these techniques see J. R. Andersen, E. M. Engler, and K. Bechgaard in the Proceedings of the New York Academy of Sciences "Conference on Synthesis and Properties of Low Dimensional Materials", New York, N.Y., June 13–16, 1977, to be published.
(48) For information on this technique see L. B. Coleman, *Rev. Sci. Instrum.*, **46**, 1125 (1975).
(49) For a description of this method as applied to the analysis of organic charge transfer complexes see ref 17a.

Oxygen-17 Magnetic Resonance Study of Oxygen Exchange between Arsenite Ion and Solvent Water

William C. Copenhafer and Philip H. Rieger*

Contribution from the Department of Chemistry, Brown University, Providence, Rhode Island 02912. *Received June 30, 1977*

Abstract: Oxygen-17 magnetic resonance spectra of aqueous solutions of sodium arsenite were measured for $0.6 < [As(III)] < 4.1$ m, $10 < t < 90$ °C. Line broadening of the water resonance in the 40–90 °C range gives the rate of oxygen exchange between $AsO(OH)_2^-$ and solvent water. Exchange takes place via a first-order pathway, $\Delta S_1^{\ddagger} = -120 \pm 3$ J K^{-1} mol^{-1}, $\Delta H_1^{\ddagger} = 25 \pm 1$ kJ mol^{-1}, and a pathway second-order in arsenite, $\Delta S_2^{\ddagger} = -102 \pm$ J K^{-1} mol^{-1}, $\Delta H_2^{\ddagger} = 33 \pm 4$ kJ mol^{-1}. Rates were measured using solutions of pH ~10.2; exchange appears to be only slightly faster in solutions of lower pH.

Introduction

Despite the use of arsenic(III) oxide, As_4O_6, by generations of analysts as a redox standard, remarkably little is known of the aqueous chemistry of As(III). Indeed, less than a decade has passed since the structures of arsenous acid and arsenite ion in aqueous media were finally established by Raman spectroscopy: trigonal pyramidal $As(OH)_3$ and $AsO(OH)_2^-$.[1,2]

An attempt was made in 1940 to measure the rate of oxygen exchange between arsenite ion and solvent water, but the exchange proved too fast for the isotopic exchange technique used.[3] Apparently because nucleophilic displacements on arsenite are very rapid, only two kinetic studies of As(III) substitution reactions have come to our attention and both involve As(III) as a catalyst: $AsO(OH)_2^-$ catalyzes the hydration of carbon dioxide,[4] and $As(OH)_3$ (and perhaps $AsO(OH)_2^-$) catalyzes the exchange of oxygen between dihydrogen arsenate, $AsO_2(OH)_2^-$, and water.[5] As the first of a series of studies of equilibria and kinetics of reactions involving As(III), we report here the measurement of the rate of oxygen exchange between arsenite ion and solvent water by ^{17}O magnetic resonance line broadening.

Experimental Section

Reagent grade sodium arsenite (Baker and Adamson) was used without purification for preparation of As(III) solutions. Analysis of this material showed that 23.6 mol % of the As(III) was present as As_4O_6, the remainder as $NaAsO_2$.

Solutions for ^{17}O NMR spectra were prepared on a vacuum line. A weighed amount of dry sodium arsenite was placed in one section of a Y-shaped sample tube. An aliquot of sodium hydroxide or *p*-toluenesulfonic acid solution was pipetted into the other section of the sample tube and the water pumped off. About 2 g of ^{17}O-enriched water (ca. 5% enrichment) was then distilled under vacuum into the sample tube. The ^{17}O water reservoir was weighed before and after the distillation so that the molal concentration of As(III) could be computed. The enriched water was recovered after running the spectra and used for subsequent samples.

^{17}O NMR spectra were recorded at 7.5 MHz (13 kG) on a Varian wide-line NMR spectrometer equipped with a 12-in. magnet and flux stabilizer. To ensure rf stability, the Varian V-4210A variable frequency unit was locked to an external frequency synthesizer (Syntest

0002-7863/78/1500-3776$01.00/0

Table I. Concentrations of As(III) Samples

Sample no.	C_{As}, m	p_α[a]	X_{acid}[b]
1	0.608	0.0318	0.08
2[c]	0.610	0.0319	0.61
3	1.11	0.0566	0.24
4	2.03	0.0989	0.10
5	3.08	0.1427	0.10
6[d]	3.08	0.1427	0.30
7	4.10	0.1814	0.09

[a] Fraction of oxygen at arsenite sites. [b] Fraction of As(III) in form of $As(OH)_3$. [c] 0.23 m in p-toluenesulfonic acid. [d] 0.20 m in p-toluenesulfonic acid.

Corp.). The sideband method of detection was employed under conditions of high frequency, low amplitude field modulation using a modulation frequency of 1000 Hz. The center band of the first ac component was rejected by detecting in phase with the modulation frequency. The two side bands served as an internal calibration for each spectrum.

Sample temperature was controlled with a Varian variable temperature accessory employing heated or cooled nitrogen and was measured by placing a copper-constantan thermocouple between the sample tube and the Dewar walls.

Viscosities and densities of arsenite solutions in normal water were measured as functions of temperature using an Ostwald viscometer and a pycnometer.

Results

^{17}O NMR spectra were measured at temperatures ranging from 10 to 90 °C for seven different samples having As(III) concentrations up to 4.10 m. Sample concentrations are given in Table I. Signal-to-noise ratios ranged from about 8:1 to more than 100:1 depending on the line width. However, only the resonance due to solvent water was observed; the arsenite ^{17}O resonance was probably too broad to be detectable. All spectra were recorded in quadruplicate; line widths were measured for each recording and averaged. Average observed line widths are given in Table II and are plotted vs. temperature in Figure 1.

The viscosities of solutions comparable to samples 3, 4, 5, and 7 were measured and fitted to the empirical equation

$$\ln (\eta/T) = \alpha + \beta/T + \gamma/T^2 \qquad (1)$$

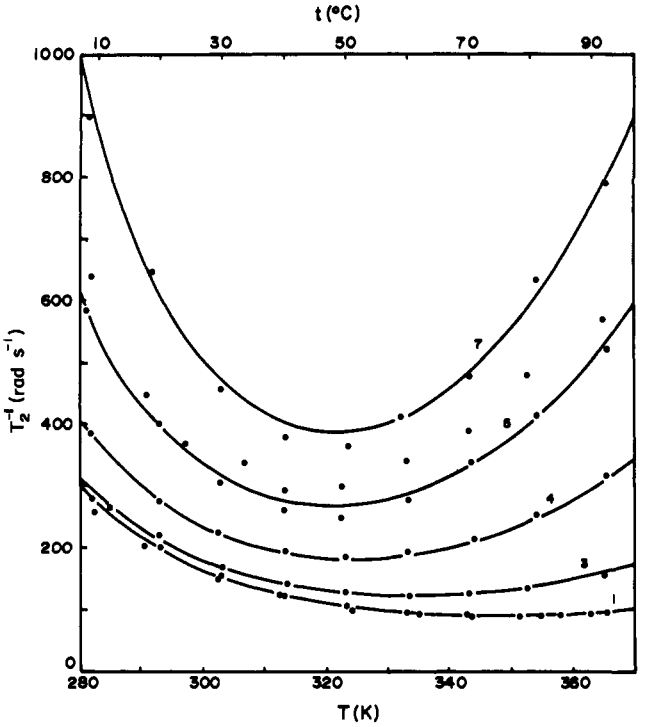

Figure 1. Measured ^{17}O NMR line widths as a function of temperature. Closed circles, samples 1, 3, 4, 5, and 7; open circles, samples 2 and 6.

by the method of least squares. The parameters α, β, and γ are given in Table III. Equation 1 and the parameters of Table III fit the measured viscosities to well within 1%, the approximate experimental uncertainty.

Assuming that oxygen exchange occurs between arsenite and solvent water, the width of the water peak is given by[6]

$$T_2^{-1} = T_{2,0}^{-1} + p_\alpha \tau_\alpha^{-1} \left(\frac{T_{2\alpha}^{-2} + (\tau_\alpha T_{2\alpha})^{-1} + \Delta\omega_\alpha^2}{(T_{2\alpha}^{-1} + \tau_\alpha^{-1})^2 + \Delta\omega_\alpha^2} \right) \qquad (2)$$

where $T_{2,0}^{-1}$ is the line width in the absence of exchange, p_α is the fraction of oxygen nuclei at arsenite sites, τ_α is the life-

Table II. ^{17}O NMR Line Widths[a]

T, K	T_2^{-1}	T, K	T_2^{-1}	T, K	T_2^{-1}	T, K	T_2^{-1}
Sample no. 1		Sample no. 2		Sample no. 3			
281.9	278 ± 9	282.5	257 ± 22	285.0	265 ± 12		
293.4	203 ± 5	290.7	204 ± 14	293.0	220 ± 5		
303.2	154 ± 5	303.2	150 ± 4	303.2	168 ± 2		
313.4	122 ± 3	313.2	123 ± 4	313.7	139 ± 3		
324.5	98 ± 5	323.3	105 ± 5	323.1	126 ± 5		
335.1	92 ± 2	333.3	92 ± 2	333.5	121 ± 2		
343.6	87 ± 2	343.4	89 ± 1	343.4	123 ± 2		
355.0	87 ± 1	351.5	87 ± 2	352.8	137 ± 3		
365.7	94 ± 2	358.2	89 ± 2	365.3	155 ± 8		
		363.1	93 ± 2				
Sample no. 4		Sample no. 5		Sample no. 6		Sample no. 7	
283.0	385 ± 12	281.2	582 ± 17	282.2	642 ± 30	281.7	900 ± 39
293.1	275 ± 10	293.1	402 ± 17	291.1	448 ± 23	292.3	650 ± 18
302.6	226 ± 8	302.9	305 ± 10	297.2	367 ± 21	303.1	456 ± 22
313.5	195 ± 6	313.4	262 ± 12	306.7	339 ± 7	313.7	378 ± 5
323.3	185 ± 6	322.6	250 ± 15	313.4	292 ± 10	323.9	363 ± 4
333.4	192 ± 2	333.5	276 ± 4	322.6	300 ± 12	332.4	410 ± 11
344.1	214 ± 7	343.9	338 ± 12	333.3	341 ± 12	343.5	477 ± 11
354.3	252 ± 12	354.3	411 ± 5	343.2	389 ± 26	354.3	633 ± 5
365.5	315 ± 11	365.7	519 ± 15	352.8	478 ± 18	365.7	788 ± 21
				365.1	568 ± 17		

[a] In units of rad s^{-1}.

Table III. Empirical Viscosity Parameters[a]

C_{As}, m	α	$10^{-3}\beta$	$10^{-6}\gamma$
1.02	−13.978	−1.459	0.574
2.03	−13.967	−1.433	0.598
3.05	−12.806	−2.164	0.747
4.07	−11.774	−2.830	0.892

[a] For η in units of kg m^{-1} s^{-1} and T in K, see eq 1.

Table IV. Least-Squares Line Width Parameters[a]

Sample no.	$10^{-5}A$, m kg^{-1} K^{-1}	$\Delta S^{\pm}$, J K^{-1} mol^{-1}	$\Delta H^{\pm}$, kJ mol^{-1}
1	296 ± 3	−104 ± 12	30 ± 4
2	273 ± 3	−134 ± 6	19 ± 2
3	425 ± 5	−106 ± 6	28 ± 2
4	377 ± 2	−103 ± 1	28 ± 1
5	353 ± 6	−95 ± 4	31 ± 1
6	379 ± 14	−104 ± 7	27 ± 3
7	352 ± 8	−93 ± 5	31 ± 2

[a] See eq 4.

time of an oxygen nucleus at an arsenite site, $T_{2\alpha}$ is the transverse relaxation time of an oxygen nucleus at an arsenite site, and $\Delta\omega_\alpha$ is the chemical shift, relative to water, of oxygen at an arsenite site.

In the slow exchange limit, where τ_α^{-1} is small compared with either $T_{2\alpha}^{-1}$ or $|\Delta\omega_\alpha|$, eq 2 reduces to

$$T_2^{-1} = T_{2,0}^{-1} + p_\alpha \tau_\alpha^{-1} \quad (3)$$

Values of τ_α^{-1}, obtained assuming the validity of eq 3, range up to about 4×10^3 s^{-1}. $T_{2\alpha}^{-1}$ is certainly greater than $T_{2,0}^{-1}$, but it seems unlikely to be even as large as τ_α^{-1}, at least at the higher temperatures. Thus the validity of eq 3 relies on the assumption that $|\Delta\omega_\alpha| \gg \tau_\alpha^{-1}$. Oxy anion ^{17}O chemical shifts are generally downfield from water by 200 ppm or more;[7] thus at 7.5 MHz, $|\Delta\omega_\alpha|$ is probably greater than 10^4 rad s^{-1}. However, if the arsenite chemical shift is as small as −200 ppm, τ_α^{-1} could be underestimated by as much as 25%.

In the concentration range studied, 0.6–4.1 m, the solution viscosity is strongly dependent on arsenite concentration, so that $T_{2,0}^{-1}$ cannot be measured independently on arsenite-free solutions. Thus, as a first step in the data analysis, it was assumed that $T_{2,0}^{-1}$ is proportional to η/T and that τ_α^{-1} is given by an absolute rate theory expression. The measured line widths were then fitted to the equation

$$T_2^{-1} = A(\eta/T) + p_\alpha(k_B T/h) \exp(\Delta S^{\pm}/R) \exp(-\Delta H^{\pm}/RT) \quad (4)$$

by a nonlinear least-squares procedure. The resulting least-squares parameters (A, $\Delta S^{\pm}$, and $\Delta H^{\pm}$) are given in Table IV. The variation in the values of A probably reflects (1) contributions to the viscosities from acid or base added to the NMR samples and (2) possible errors in extrapolation of viscosities for samples 1 and 2, which lie somewhat outside the range of the viscosity measurements. The temperature dependence of η/T should be nearly correct, however, and the low-temperature fit is well within experimental error in all cases. The parameter A is determined primarily by the low-temperature points and is relatively independent of the kinetic parameters. Although the fit to the high-temperature points is good as well, the activation parameters neither are constant nor do they exhibit any sensible trend.

Assuming that $A(\eta/T)$ is a good approximation to $T_{2,0}^{-1}$, τ_α^{-1} can be computed from eq 3. These values of τ_α^{-1}, *which may be regarded as pseudo-first-order rate constants,* are plotted against the concentration of As(III) for samples 1, 3, 4, 5, and 7 in Figure 2 for data at 40 °C and above (60 °C and above for sample 1; the kinetic contribution to the line widths is negligible at lower temperatures). As is seen, there is an excellent linear correlation between τ_α^{-1} and arsenic concentration, suggesting that both first-order and second-order exchange pathways are important. Indeed, absolute rate theory plots (Figure 3) of the intercepts (k_1 with units of s^{-1}) and the slopes (k_2 with units of m^{-1} s^{-1}) of Figure 2 give satisfactory straight lines and activation parameters: $\Delta S_1^{\pm} = -120 \pm 3$ J K^{-1} mol^{-1}, $\Delta H_2^{\pm} = 25 \pm 1$ kJ mol^{-1} for the first-order process; $\Delta S_2^{\pm} = -102 \pm 10$ J K^{-1} mol^{-1}, $\Delta H_2^{\pm} = 33 \pm 4$ kJ mol^{-1} for the second-order process. These parameters can, of course, be used to compute τ_α^{-1} and, together with the values of A given in Table IV, are responsible for the solid curves of Figure 1. It should be noted that if systematic error due to the approximate nature of eq 3 is significant, then values of τ_α^{-1} for the high-concentration, high-temperature points are underestimated; thus, if anything, the second-order pathway is even more important, the activation enthalpy may be larger than 33 kJ mol^{-1}, and the activation entropy may be less negative than −102 J K^{-1} mol^{-1}.

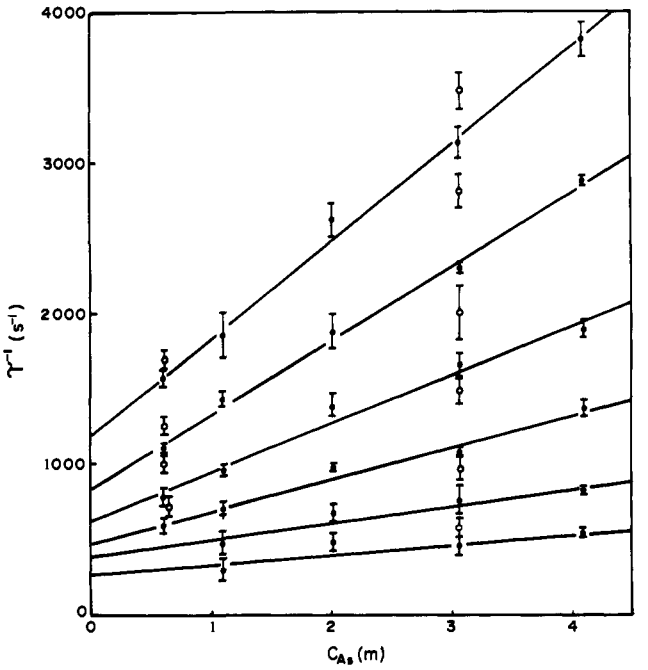

Figure 2. Observed rate constants, τ_α^{-1}, as a function of total As(III) concentration at six temperatures. Closed circles and straight lines, samples 1, 3, 4, 5, and 7; open circles, samples 2 and 6.

Values of τ_α^{-1} for samples 2 and 6, which were slightly acidified with *p*-toluenesulfonic acid, and thus had significant concentrations of $As(OH)_3$, are also plotted in Figure 2 but were not included in the least-squares fit resulting in the straight lines of the figure. It is apparent that oxygen exchange is somewhat faster in the more acidic solutions, and the rather limited data available suggest that exchange with $As(OH)_3$ is faster than with $AsO(OH)_2^-$ by a factor of 3 or 4. However, because of the low solubility of As_4O_6, the experiments could not be extended to lower pH, and the data are not sufficiently accurate to establish a rate law which distinguishes between $As(OH)_3$ and $AsO(OH)_2^-$. The results presented here thus refer, within reasonable error limits, to exchange between water and $AsO(OH)_2^-$.

Discussion

The observed first-order oxygen exchange process presumably corresponds to a nucleophilic displacement by water on arsenite. Entropies of activation for bimolecular nucleophilic

Table V. Rate Constants for Oxygen Exchange at 30 °C

Reactants	k	Ionic strength	Ref
$AsO_4^{3-} + H_2O$	1.5×10^{-6} s^{-1}	0.55	11
$AsO_3(OH)^{2-} + H_2O$	1.2×10^{-5} s^{-1}	0.55	11
$AsO_2(OH)_2^- + H_2O$	1.0×10^{-4} s^{-1}	0.55	11
$AsO(OH)_2^- + H_2O$	167 s^{-1}		This work
$AsO_3(OH)^{2-} + AsO_3(OH)^{2-}$	8.5×10^{-6} M^{-1} s^{-1}	0.55	11
$AsO_3(OH)^{2-} + AsO_2(OH)_2^-$	6.4×10^{-3} M^{-1} s^{-1}	0.55	11
$AsO_2(OH)_2^- + AsO_2(OH)_2^-$	7.4×10^{-2} M^{-1} s^{-1}	0.55	11
$AsO_2(OH)_2^- + As(OH)_3$	6.8 M^{-1} s^{-1}	0.20	5
$AsO_2(OH)_2^- + AsO(OH)_2^-$	<7 M^{-1} s^{-1}	0.20	5
$AsO_3(OH)^{2-} + As(OH)_3$	$<2 \times 10^{-2}$ M^{-1} s^{-1}	0.20	5
$AsO(OH)_2^- + AsO(OH)_2^-$	69 m^{-1} s^{-1}		This work

displacement reactions in aqueous solution are typically on the order of −50 to −70 J K^{-1} mol^{-1},[8] considerably less negative than the value found in this case, −120 J K^{-1} mol^{-1}. This suggests that an additional solvent molecule may be involved. Indeed, nucleophilic displacements known to be termolecular have entropies of activation in the range −90 to −140 J K^{-1} mol^{-1}.[9] Involvement of a second water molecule undoubtedly facilitates proton transfer in a transition state which we formulate as

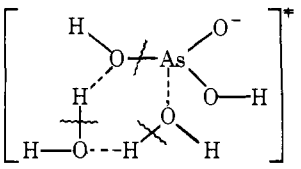

The second-order oxygen exchange pathway must correspond to the process

$$2AsO(OH)_2^- \underset{k_{-2}}{\overset{k_2}{\rightleftharpoons}} H_2O + As_2O_3(OH)_2^{2-} \qquad (5)$$

The entropy of activation for the second-order process. −102 ± 10 J K^{-1} mol^{-1}, is subject to some uncertainty and could be rather less negative if the chemical shift of arsenite oxygen is on the order of −200 ppm (see discussion in Results section). It would appear therefore that the process is most likely a bimolecular nucleophilic attack of arsenite on arsenite to form an oxo-bridged dimer. Since the Raman studies of Loehr and Plane[1] failed to produce evidence of condensed arsenites at concentrations up to 5 M, the equilibrium constant for reaction 5 must be less than about 0.01 and the hydrolysis rate constant, k_{-2}, therefore greater than about 7×10^3 s^{-1} at 30 °C. This rate is considerably faster than the first-order rate of oxygen exchange at that temperature, $k_1 = 167$ s^{-1}, presumably reflecting the fact that arsenite is a better leaving group than hydroxide and suggesting that extra solvent participation may not be required. A similar effect is seen in the corresponding As(V) case. The rate of hydrolysis of pyroarsenate $As_2O_6(OH)^-$ is about 0.06 s^{-1} at 30 °C,[10] almost three orders of magnitude faster than the first-order rate of oxygen exchange with $AsO_2(OH)_2^-$ (see Table V).

The rate law found for oxygen exchange with arsenite is reminiscent of the results of a recent study of oxygen exchange with arsenate(V).[11] The rate constants for the various pathways found in the latter case are given in Table V along with the rate constants for arsenite oxygen exchange extrapolated to 30 °C. Both first- and second-order processes for arsenate are very much slower than for arsenite. The difference is attributable mostly to significantly larger enthalpies of activation in the case of arsenate, confirming the expectation that As(V)-O bonds are significantly stronger than the corresponding As(III)-O bonds.

Of considerable interest is the observation that the arsenate exchange process is catalyzed by As(III).[5] The rate constant,

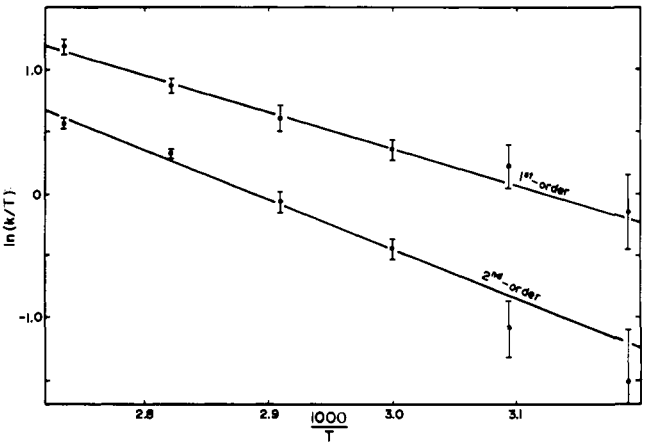

Figure 3. Absolute rate theory plot of first- and second-order rate constants. The straight lines are least squares fitted to the points with weights inversely proportional to the variances.

6.8 M^{-1} s^{-1} (30 °C), for the pathway $AsO_2(OH)_2^-$ + $As(OH)_3$ (and the probably somewhat smaller rate constant for the pathway $AsO_2(OH)_2^-$ + $AsO(OH)_2^-$) seem to be significantly smaller than the second-order arsenite oxygen exchange rate, about 70 m^{-1} s^{-1}, at the same temperature. Arsenite must be the nucleophile in both cases, but the substrate is arsenate in one instance and arsenite in the other. Again the relative strengths of the As(V)-O and As(III)-O bonds are significant. This is reflected by the enthalpies of activation: about 50 kJ mol^{-1} for the arsenite-arsenate reaction compared with 33 kJ mol^{-1} for the arsenite-arsenite reaction.

Arsenite ion is known to catalyze the hydration of carbon dioxide:

$$CO_2 + H_2O \xrightarrow{AsO(OH)_2^-} H_2CO_3$$

This process is first order in both CO_2 and $AsO(OH)_2^-$ with a rate constant at 0 °C of about 4 M^{-1} s^{-1}.[4] The probable mechanism of the reaction is[12] given in eq 6 and 7. Assuming

$$AsO(OH)_2^- + CO_2 \overset{\text{fast}}{\rightleftharpoons} O_2COAs(OH)_2^- \qquad (6)$$

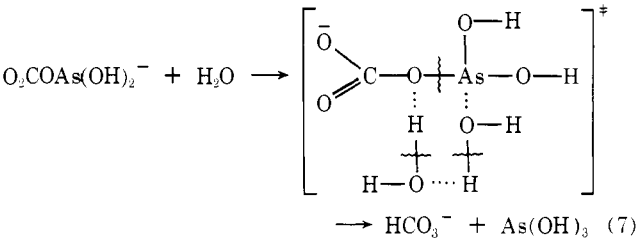

that step 6 is a fast equilibrium, the observed rate constant is $k_{obsd} = K_6k_7$. The transition state of step 7 is similar to that postulated for the first-order oxygen exchange process, but with HCO_3^- as the leaving group instead of water. The rate constant k_7 is thus expected to be somewhat smaller than k_1, the oxygen exchange constant, which is about 50 s^{-1} at 0 °C. Although the numbers are consistent with the proposed mechanism, further discussion must await the results of studies of related systems which are in progress.

Acknowledgments. Many stimulating discussions with Professor John O. Edwards and financial support from the National Institute of Environmental Health Sciences were essential to the completion of this work.

References and Notes

(1) T. M. Loehr and R. A. Plane, *Inorg. Chem.*, **7**, 1708 (1968).
(2) H. A. Szymanski, L. Marabella, J. Hoke, and J. Harter, *Appl. Spectrosc.*, **22**, 297 (1968).
(3) N. F. Hall and O. R. Alexander, *J. Am. Chem. Soc.*, **62**, 3455 (1940).
(4) A. E. Dennard and R. J. P. Williams, *J. Chem. Soc. A*, 812 (1966).
(5) A. Okumura, N. Yamamoto, and N. Okazaki, *Bull. Chem. Soc. Jpn.*, **46**, 3633 (1973).
(6) T. J. Swift and R. E. Connick, *J. Chem. Phys.*, **37**, 307 (1962).
(7) H. A. Crist, P. Diehl, H. R. Schneider, and H. Dahn, *Helv. Chim. Acta*, **44**, 865 (1961); B. N. Figgis, R. G. Kidd, and R. S. Nyholm, *Proc. R. Soc. London, Ser. A*, **269**, 469 (1962).
(8) J. O. Edwards, *J. Chem. Educ.*, **45**, 386 (1968).
(9) M. A. P. Dankleff, R. Curci, J. O. Edwards, and H.-Y. Pyun, *J. Am. Chem. Soc.*, **90**, 3209 (1968).
(10) T. G. Richmond, J. R. Johnson, J. O. Edwards, and P. H. Rieger, *Aust. J. Chem.*, **30**, 1187 (1977).
(11) A. Okumura and N. Okazaki, *Bull. Chem. Soc. Jpn.*, **46**, 2937 (1973).
(12) N. J. Fina and J. O. Edwards, *Int. J. Chem. Kinet.*, **5**, 1 (1973).

Natural Solid State Optical Activity of Tris(ethylenediamine)metal(II) Nitrates. 4. Optical Activity of $Zn(en)_3(NO_3)_2$ and Assignment of the Lowest Electronic Transition in NO_3^-

Richard Alan Palmer* and Mark Chin-Lan Yang

Contribution from the Paul M. Gross Chemical Laboratory, Duke University, Durham, North Carolina 27706. *Received September 26, 1977*

Abstract: The nature of the lowest observed electronic transition of the nitrate ion has been reinvestigated by measurement of the orthoaxial linear dichroism (LD) and axial absorption and circular dichroism (CD) of the enantiomorphous crystals of tris(ethylenediamine)zinc(II) nitrate at temperatures from ambient to 5 K. The data support the assignment of the transition as $^1A_1'' \leftarrow {}^1A_1'$ ($a_2''(\pi^*) \leftarrow a_2'(n)$). In-plane intensity in the LD spectrum is analyzed in terms of the C_{3v} symmetry of the excited state and vibronic perturbation by two ϵ modes, consistent with the vibronic structure observed at 5 K. The much stronger out-of-plane intensity is shown to be consistent with interaction between NO_3^- ions to form a dimer of D_3 symmetry.

The spontaneous resolution of tris(ethylenediamine)-zinc(II) ion in the hexagonal crystals of the nitrate salt provides a unique opportunity to observe the natural optical activity of the intrinsically achiral nitrate ion. The lowest electronic transition of NO_3^- is observed at ca. 3.3 μm^{-1}, with an absorptivity sufficiently low to be amenable to measurement in single-crystal absorption studies.[1,2] However, with the exception of $Zn(en)_3(NO_3)_2$ and its nickel(II) and cobalt(II) analogues, no other incidence of enantiomorphous uniaxial or cubic crystals of nitrate salts are known, and the brief description of the circular dichroism of the zinc crystal in the first paper of this series[3] is the only previous mention in the literature of the natural optical activity of the NO_3^- ion.

Although the 3.25 μm^{-1} band of the NO_3^- ion is also observed in the absorption and CD spectra of $Ni(en)_3(NO_3)_2$[3-5] and $Co(en)_3(NO_3)_2$,[3,6] ligand field absorption and charge transfer, respectively, partially mask its contours in these crystals. However, $Zn(en)_3(NO_2)_3$, with its d^{10} metal ion and relatively high energy charge transfer, is devoid of other absorption in the 3.0–4.0 μm^{-1} region, and thus is more suitable than the other members of the series for studying the NO_3^- band. The combination of linear and circular dichroism (LD and CD) measurements of this band at ambient and cryogenic temperatures is reported here along with discussion of its assignment in light of these results.

Experimental Section

Single crystals of $Zn(en)_3(NO_3)_2$ with dimensions perpendicular to the needle (c) axis of 2–4 mm were grown by slow evaporation of aqueous solutions. For axial spectra, sections (ca. 0.5 mm thick) were cut with a thread saw and polished on a water-dampened fine polishing cloth. The perpendicularity of the polished faces to the c axis was checked by observing the centering and perfection of the uniaxial interference figure from both directions. Orthoaxial (LD) spectra were measured on crystals as grown or polished to appropriate thickness. (ca. 0.3 mm).

Absorption spectra were measured using a Cary 14R spectrophotometer and associated accessories, and CD spectra were obtained on a Durrum-JASCO ORD/CD-5 circular dichroism recorder with SS-20 modification, all as previously described.[7,8]

Values of $\Delta\epsilon$ were derived from the instrumental data by the relationship $\Delta\epsilon = \phi(33cl)^{-1}$, where ϕ is the ellipticity in degrees taken from the chart, c is the molar concentration, and l is the path length (cm). (The output of the JASCO instrument with the SS-20 modification is in degrees ellipticity.) The instrument was standardized against d-10-camphorsulfonic acid, for which the most recent and reliable value for $[\theta] = [\phi]M \times 10^{-2} = 3300\Delta\epsilon$, is given by Wong[9] as +7260 deg cm^2 $dmol^{-1}$. Formulas used for calculation of I, D, R, and g have been given previously.[6]

Results

Spectral results in terms of the integrated band intensity (I), dipole strength (D), rotational strength (R), and anisotropy factor (g) are given in Tables I and II. The strong temperature dependence of intensity in both absorption and CD should be noted. In addition, all spectra exhibit well-developed progressions of vibronic structure at liquid helium temperature (5 K), as shown in Figures 1 and 2. Table III lists the energies

0002-7863/78/1500-3780$01.00/0